Electro-Cycle: Employing Leg EMG to Classify Bicycle Resistance

Alexander Dyer[1], Haley Kwoun[1]
[1]Harvard School of Engineering and Applied Sciences

ACRM
AMERICAN CONGRESS OF REHABILITATION MEDICINE

Harvard John A. Paulson School of Engineering and Applied Sciences

Introduction

Utilizing the correct bicycle gear during biking is critical to muscular efficiency [1]. **Individuals with upper-body complications**, such as amputees, **have difficulty adjusting bike gears**, reducing their ability to switch to the appropriate gear while pedaling at a constant cadence [2]. **Typical bike equipment does not provide any mechanisms to assist in automatic gear switching**, thereby **reducing the accessibility of cycling as a therapeutic modality** with upper- and lower-body complications, such as paresis [3].

Primary Aims

1. Determine Ideal Electrode Placement during Biking to **Capture EMG from the Rectus Femoris and Gastrocnemius**.
2. Develop a **Signal Processing Pipeline** to Transform the EMG Data into Windows Reflective of the **Pedal Cycle**.
3. Analyze EMG Data with **K-Nearest Neighbor and Linear Discriminant Analysis to Classify Environmental Resistance**.

Data Methodology

Overview: The Olimex Shield Device relays EMG recordings into the Arduino. The subject cycles on a stationary bike with various resistance levels, ranging from 1 through 12 (a higher value indicates increased resistance).

Electrode Validation: The electrodes are placed to capture either the rectus femoris or the gastrocnemius per literature-suggested locations. This placement is verified by evaluating the SNR across a 10-minute cycle.



Figure 1. Subject on Stationary Bike with Rectus Femoris Electrodes (Right Image Adapted from [4])

References

[1] C.-L. Chen and M.-C. Tsai, "Torque control of power-assisted bike via planetary gear mechanism," in 2017 20th International Conference on Electrical Machines and Systems (ICEMS), pp. 1–5, Aug. 2017.
[2] V. Dimitrov, "Overview of the Ways to Design an Electric Bicycle," in 2018 IX National Conference with International Participation (ELECTRONICA), pp. 1–4, May 2018
[3] H. Mohammadi-Abdar, A. L. Ridgel, F. M. Discenzo, and K. A. Loparo, "Design and Development of a Smart Exercise Bike for Motor Rehabilitation in Individuals With Parkinson's Disease," IEEE/ASME Transactions on Mechatronics, vol. 21, pp. 1650–1658, June 2016. Conference Name: IEEE/ASME Transactions on Mechatronics.
[4] "File:Rectus femoris.png - Wikimedia Commons," Wikimedia.org, 2022. https://commons.wikimedia.org/wiki/File:Rectus_femoris.png (accessed December 03, 2023).

Scan for Abstract and More Information

Data Processing Results

Methodology: Data cleaning involved adding a constant offset to the signal to obtain a **zero-mean EMG**. The signal was then filtered using a **fourth-order bandpass Butterworth filter with poles at 5 and 400 Hz**. Enveloping involved a **second-order low-pass Butterworth filter with a pole at 10 Hz**. This processed EMG was then windowed using **peak detection** and verified with the times recorded for each pedal cycle.

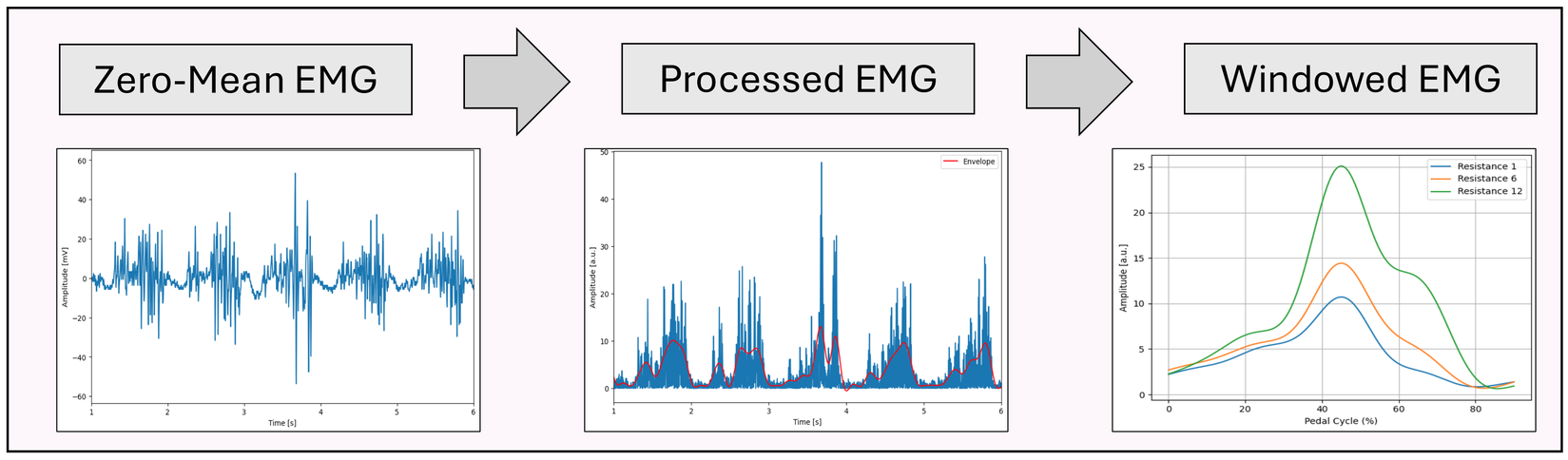


Figure 3. Data Processing Pipeline

K-Nearest Neighbor Results

Methodology: Determine the accuracy of predicting the resistance associated with EMG data from one pedal cycle for various resistances. **KNN predicts the resistances by calculating the signal similarity** between a given signal and the mean signal for each resistance, as determined by the training data.

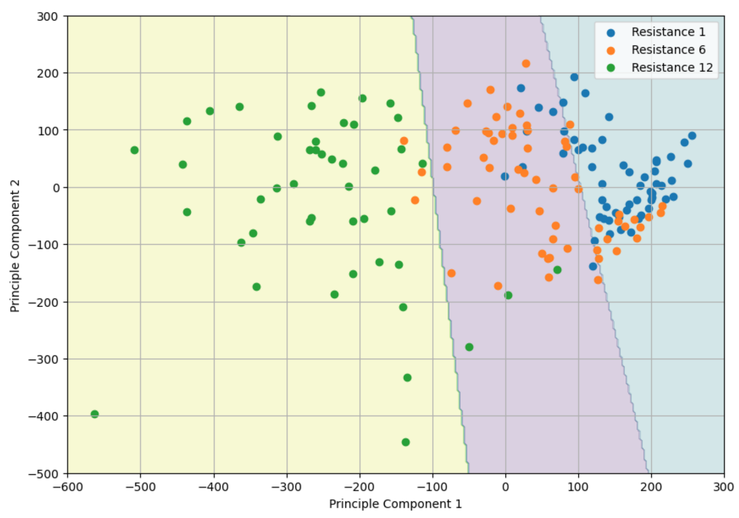


Figure 4. KNN Decision Boundaries Overlaid on Rectus Femoris Principal Component Analysis (PCA)

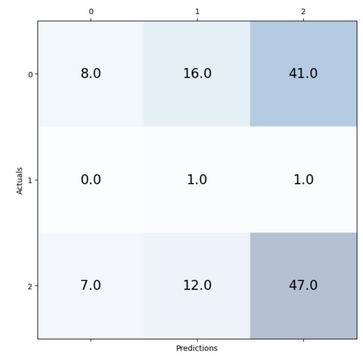


Figure 5. Confusion Matrix of Gastrocnemius EMG KNN

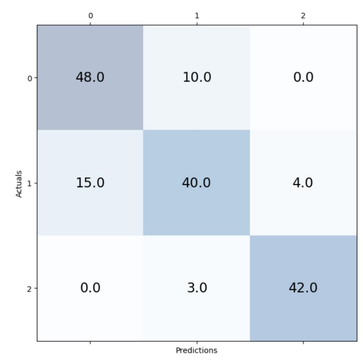


Figure 6. Confusion Matrix of Rectus Femoris EMG KNN

Linear Discriminant Analysis Results

Methodology: Given the low accuracy of KNN for gastrocnemius, only rectus femoris EMG was employed for linear discriminant analysis (LDA). LDA calculates the Fisher boundary between two samples, **incorporating information on within and between-class variation.**

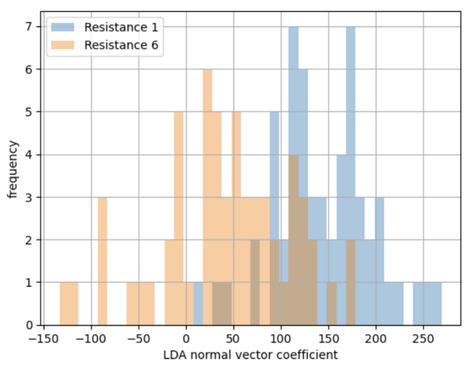


Figure 7. Histogram of Fisher Projections of Rectus Femoris EMG at Resistances 1 and 6

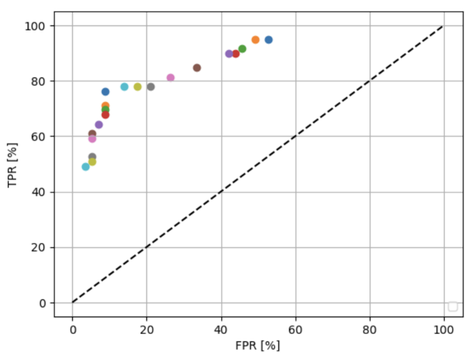


Figure 8. Receiver Operating Curve (ROC) of Rectus Femoris EMG. True Positive Rate (TPR) and False Positive Rate (FPR) Displayed Axes.

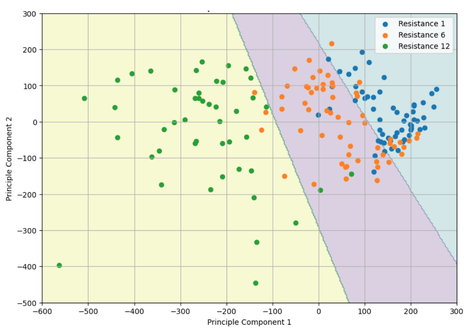


Figure 9. LDA Decision Boundaries Overlaid on Rectus Femoris Principal Component Analysis (PCA)

Conclusions

- **>80% Accuracy for both LDA and KNN** using Rectus Femoris EMG.
- Gastrocnemius Has Low Accuracy.
- **LDA and KNN** Converge to Similar Boundaries.

Future Work

- Engineer **Wearable Hardware Platform** Integrated with Bike Gear Mechanism.
- Employ **Validation on More Subjects**.
- Employ Subjects with **Clinically Documented Abnormalities**.